NJC

One-step synthesis of structure controlled vinyl functionalized hollow mesoporous silica nanospheres

Journal:	*New Journal of Chemistry*
Manuscript ID:	NJ-ART-07-2014-001132.R2
Article Type:	Paper
Date Submitted by the Author:	09-Oct-2014

Complete List of Authors:	li, jie; School of Materials Science and Engineering, Wuhan University of Technology, Chen, Lianxi; School of chemical and life science, Wuhan University of Technology, Li, Xi; School of chemical and life science, Wuhan University of Technology Wuhan, Zhang, Chao; Wuhan University of Technology, Jiang, Yang; School of chemical and life science, Wuhan University of Technology Wuhan,

One-step synthesis of structure controlled vinyl functionalized hollow mesoporous silica nanospheres

Jie Li, [ab] Lianxi Chen,[*a] Xi Li, [a] Chaocan Zhang [b] and Yang Jiang [a]

([a] School of Chemistry, Chemical Engineer and Life Science, Wuhan University of Technology, Wuhan, 430070, PR China. [b] School of Materials Science and Engineering, Wuhan University of Technology, Wuhan, 430070, PR China)

In the present study, vinyl functionalized hollow mesoporous silica nanospheres (V-HMSNSs) with tailored mesostructure have been successfully synthesized via one-step synthetic strategy using cation surfactant cetyltrimethylammonium bromide (CTAB) as a single micelle template, vinyltriethoxysilane (VTES) as precursor. It was demonstrated, for the first time, that V-HMSNSs with controllable mesostructure can be easily obtained by adjusting concentration of CTAB at aqueous solution under low amount of ammonia. Only solid spheres including vinyl functional groups were generated below the critical micelle concentration value (CMC, 0.0009 M) of CTAB. However, the nanosphers or nanorods with hollow mesostructure were obtained at this value or above it (0.005 M). Whereas, no particles were generated at higher concentration of CTAB (0.008 M or more than it). It was suggested that the formation of CTAB micelles was closely related with the formation of V-HMSNSs. In addition, the V-HMSNSs with well-defined mesostructure would be obtained as the volume ratio of alcohol to water was about 25:25. More importantly, from these investigations, it appeared that the synthetic method should be highly flexible and enable uniform distribution of functional groups within mesoporous silica frameworks.

Introduction

There has been growing interest in the past decade in fabricating organic-inorganic hybrid silica materials, among these hybrid materials, a typical and important class of silica materials is hollow mesostructure silica material. So far, hollow mesoporous hybrid silica materials with various nanostructure have been synthesized, such as nanospheres, nanotubes or nanorods and other nanoporous structures, etc., due to their low density, low toxicity, high biocompatibility, large specific surface areas and excellent thermal and mechanical stability, and thus have been widely applied in the fields of catalysis, separation/adsorption, biomedicine and controlled release of

drugs.[1-7]

The discovery of the M41S silica families by Mobil scientists in 1992 opened up an era of new inorganic materials with ordered mesopore structure by using organic templates as structuredirecting agents.[8-9] On this basis, for more than several years, many researchers have applied themselves to investigating the organic functionalized hollow mesoporous silica nanospheres (OHMSNs). Compared with traditionally inorganic silica hollow mesoporous nanospheres, OHMSNs combine the advantages of organic chemistry and inorganic building blocks. Except that they are more active and more easily modified by chemical transformation of the organic groups in the hybrid silica networks.[10-15] Especially, the preparation of OHMSNs has attracted much attention because of their excellent properties and potential applications. By now, there are two common synthesis approaches for OHMSNs, called post-grafting and co-condensation synthesis.[16-26] For the former method, organic groups were directly grafted onto the pore surface of pure hollow mesoporous silica materials. It may often lead to a nonhomogeneous distribution of the organic groups within the pores and a lower degree of occupation. In extreme cases (e.g., with very bulky grafting species), complete closure of the pores can be caused (pore blocking). For another method, co-condensation synthesis, also known as direct synthesis or one pot synthesis, is an alternative method, involving the simultaneous condensation of corresponding silica and organosilica precursors.[16,20,27-29] However, in this case, the content of organic functionalities in the mixture does not exceed 40 mol%, furthermore, the proportion of terminal organic groups that are incorporated into the pore-wall network lower than would correspond to the starting concentration of the reaction mixture.

In this study, a facile and low cost synthetic strategy has been adopted for preparation of OHMSNs. To our knowledge, the key point of this method lies in organic functional groups existing in the entire silica networks including inner core and outer shell. And more importantly, compared with the former two methods it offers a higher and more uniform surface coverage of functional groups and a better control of the surface properties of the resultant materials. In this paper, structure controlled vinyl functionalized hollow mesoporous silica nanospheres (V-HMSNSs) were successfully synthesized via one-step method using CTAB as template, VTES as precursor. It was found that the concentrations of CTAB plays an important role in the mesostructure and morphology formation of the samples at pure water solution.

Experimental Section

Chemicals and Reagents

Vinyltriethoxysilane (VTES, 99%) was purchased from Aladdin. Aaqueous ammonia solution (28 wt%), cetyltrimethylammonium bromide (CTAB), and other reagents were were obtained from Sinopharm Chemical Reagent Company Ltd. (China). All materials were of analytical grade and were used without further purification. Deionized water was prepared in our laboratory.

Synthesis Procedure

Synthesis of V-HMSNSs in Aqueous Solution Using Ammonia as the Catalyst. In a typical synthesis procedure, (0.016 g, 0.05 g, 0.1 g, 0.2 g) of CTAB and (1 mL, 2 mL, 3 mL) aqueous ammonia solution were dissolved in 50 mL of water. After the surfactant was fully dissolved, 1.8 g of VTES was dropwise added into the solution with vigorous stirring at room temperature (25 ^{o}C). The molar ratio of the reactants was VTES/CTAB/NH_3/H_2O= 1:(0.0045-0.057):(5.6-17):287. The resultant mixture was stirred at the same temperature for additional 3 h, the solid product was recovered by filtration and air-dried at room temperature overnight. Finally, in order to completely remove the surfactant, 1.0 g of as-synthesized material was extracted by refluxing in certain amount of ethanol containing concentrated aqueous HCl solution for 24 h. The extracted sample was vinyl-functionalized hollow mesoporous silica nanoparticles.

Synthesis of V-HMSNSs in Alcohol/Water Solution Using Ammonia as the Catalyst. The synthesis procedure is similar to V-HMSNSs in aqueous solution, except that alcohol water mixture as a solvent. The molar ratio of the reactants was VTES/CTAB/NH_3/EtOH/H_2O= 1:0.057:5.6:(0-90):(294-0).

Characterization methods

Transmission electron microscopy (TEM) (JEM-2100F STEM/EDS) was used for observing the morphology and measuring the geometric parameters of the particles. In addition, the average diameters of the samples were defined by statistics $\bar{x} = \sum_{i=1}^{n} x_i \Big/ n$. Where x_i is the diameter gained by measuring n spheres (n≥5) for each sample using TEM, and $\bar{x}$ was the average particles size. The samples were prepared by dipping a carbon coated copper grid, and evaporating the ethanol solvent. Fourier transform

infrared (FTIR) spectra were collected with a Nicolet Nexus 470 IR spectrometer with KBr pellet. Thermogravimetric Analysis (TGA) was carried out on TG 209 instrument to determine the thermal stability of the samples, and the heating rate was 25 ^{o}C/min from 25 to 1000 ^{o}C under room atmospheric pressure. X-ray photoelectron spectroscopy (XPS) (VG Multilab 2000) was used to provide information on organic groups coverage on surface. The nitrogen adsorption experiment was performed at 77 K on Micromeritics ASAP 2020 system. Prior to the measurement, the samples were outgassed at 150 ^{o}C for 7 h. The Brunauer-Emmett-Teller (BET) specific surface areas were calculated using adsorption data. The total pore volumes were estimated from the amounts adsorbed at highest relative pressure (P/P_0) for each sample (P/P_0=0.99). Pore size distributions were calculated from the adsorption branch using the Barrett-Joyner-Halenda (BJH) method.

Results and Discussion

The formation mechanism of V-HMSNSs

A fundamental condition for the synthesis of V-HMSNSs was that an attractive interaction between the template and the silica precursor was produced to ensure inclusion of the structure director without phase separation taking place. According to the suggestion of Huo et al.,[30-31] if the reaction was taken place under basic conditions (whereby the silica species were present as anions) and cationic quaternary ammonium surfactants were used as the structure-directing agent (SDA), the synthetic pathway was termed $S^{+}I^{-}$ (S: surfactant ; I: inorganic species). In this study, V-HMSNSs were obtained using this synthetic strategy, the typical synthesis of V-HMSNSs was schematically illustrated in Scheme 1. A vinyl functionalized silica shell was directly formed on the surface of each CTAB micell by the hydrolysis and condensation of VTES with the aid of ammonium catalyst, forming core-shell structure, denoted as CTAB@V-SiO_2. Finally, cationic surfactants CTAB cores were extracted completely to synthesize V-HMSNSs by using certain amount of ethanol containing concentrated aqueous HCl solution.

Effect of the concentrations of CTAB

It has been well known that CTAB was not only acted as a template, but also acted as a surfactant. The vinyltriethoxysilane precursor can form an emulsion with the aid of surfactant, which favored the hydrolysis and condensation of VTES precursor at

aqueous solution. Therefore, the influence of different concentrations of CTAB on the formation of V-HMSNs has been investigated at aqueous solution using ammonia as the catalyst. As listed in Table 1. It was found that no particles were produced until the concentration of CTAB was reduced to 0.005 at aqueous solution. Fig.1 gave the TEM images of samples synthesized with different concentrations of CTAB: (A, B) = 0.0005 M, (C, D)= 0.0009 M and (E, F)= 0.005 M at aqueous solution, in which Fig.1(A), (C) and (E) meant low magnification of TEM images, and Fig.1(B), (D) and (F) referred to corresponding high magnification of TEM images. It was clearly observed that the solid nanospheres were changed into hollow mesostructure as the concentration of CTAB was increased from 0.0005 to 0.0009 M. And more interestingly, the coexistence of nanospheres and nanorods with hollow mesostructures was occurred when the concentration of CTAB was up to 0.0009 M (Fig.1(C, D)). While the CTAB concentration was further increased to 0.005 M, the completely viny functionalized hollow mesoporous silica nanorods can be obtained (Fig.1(E, F)). Based on the previous reports, it was well known that the critical micelle concentration (CMC) of CTAB at aqueous solution was about 0.0009 M.[32-33] So it was not difficult to understand that single micelles were formed when the concentration of CTAB was lower than 0.0009 M, resulting in hydrolysis and condensation alone of VTES and forming solid spheres, as shown in Fig.1(A, B). While the concentration of CTAB was increased to its CMC value, the single micelles may be aggregated into large rod-like micelles, which favored the inclusion of CTAB by VTES molecules, led to the generation of finally hollow mesostructure, just as indicated in Fig.1(C, D). And with the CTAB concentration further increased, a larger aggregates of micelles were formed, resulting in the formation of rod-like micelles, and then VTES molecules were hydrolyzed and condensed around the surface of rod-like micelles. Consequently, rod-like hollow mesostructure were completely generated, as shown in Fig.1(E, F). Furthermore, in order to characterize the structure and component of V-HMSNs, the FTIR spectra of (a) CTAB, (b) CATB@V-SiO_2, (c) V-HMSNs and (d) pure silica nanospheres were compared, as shown in Fig.2. For CATB@V-SiO_2 (Fig.2(b)), bands observed at 2921 cm^{-1} and 2839 cm^{-1} were attributed to CTAB, which were assigned to asymmetric (2921 cm^{-1}) and symmetric (2839 cm^{-1}) stretching vibrations of C-CH_2 in the methylene chains (Fig.2(a)). However, for V-HMSNs (Fig.2(c)), no absorption peaks were observed at this range. In addition, the characteristic peaks of V-HMSNs can be clearly found as compared

with the typical spectrum of standard pure silica nanospheres, such as the peaks at 3064, 3019 and 2965 cm^{-1} was assigned to stretching vibrations of =CHx in the V-HMSNs frameworks. Also the strong amplitudes of Si-O-Si at 1096 cm^{-1} in pure silica networks (Fig.2(d)) was split into two peaks (1046 and 1134 cm^{-1}) in V-HMSNs.[34] The results of FTIR spectra fully illustrated that CTAB was completely removed from V-HMSNs through extraction, besides, vinyl groups were existed in the structure of V-HMSNs. In addition, in order to indicate the distribution and the percentage of the organic groups in samples, Fig.3b presented the TGA curve of V-HMSNSs synthesized in this study. In comparison, the TGA curve of pure silica nanoparticles was also given, as shown in Fig.3(a). There was no obvious weight loss in the entire TGA process, except that weight loss in the range of 30-160 ^{o}C due to evaporation of surface physical water. However, For the V-HMSNSs, the TGA process can be provided four main stages (Fig.3b). In the first stage (30–180 ^{o}C), the weight was almost unchanged, which indicated the V-HMSNSs have no obvious physical/chemical change. In the second stage (180–250 ^{o}C), the weight was increased by 7.3 %, which revealed that the oxidation of vinyl groups.[35] In the third stage (250–450 ^{o}C), the weight was sharply decreased as the increment of temperature, indicating that the oxides may be further changed into CO_2 which resulting in weight loss. In the four stage (450–800 ^{o}C), the weight was declined slowly. While the temperature was above 800 ^{o}C, the weight was nearly unchanged. Meanwhile, the surface chemical composition of the V-HMSNSs was determined by XPS. Fig. 4b shows a typical XPS survey spectrum of the pure silica surface. The characteristic signals for pure silica (Si2p at 103 eV and Si2s at 155 eV) and oxygen (O1s at 531.8 eV) are clearly detected. An additional carbon signal (C1s at 285 eV) is also detected, duo to the interference of unavoidable contamination of pure silica during analysis.[36-37] Comparatively, for V-HMSNSs, characteristic signals attributed to silicon, oxygen and additional signals assigned to C1s at 285 eV, and the carbon signal is noticeably stronger compared with the pure silica surface, as shown in Fig.4(a), due to the additional carbon in the V-HMSNSs frameworks. Besides, the ratio of C1s/ O1s of V-HMSNSs, compared with the pure silica nanoparticles, was increased from 3/61 to 42/22, it is suggests that a large number of hydroxyl groups in the pure silica is replaced by vinyl group in V-HMSNSs.

To better understanding the the effect of CTAB concentration on the formation of mesostructure, N_2 adsorption-desorption measurements were carried out on the

products synthesized at aqueous solution using different concentrations of CTAB. Fig.5 showed the representative N_2 adsorption-desorption isotherms and the corresponding pore size distributions of the samples whose TEM images were displayed in Fig.1(C, D) and (E, F). From N_2 adsorption-desorption isotherms, it was found that all of these two samples exhibited a typical □isotherm, these behaviors illustrated that the shells on the surface of obtained V-HMSNSs were porous as well as a very broad distributions of these pores. The pore size distributions of obtained V-HMSNSs were calculated by the BJH method from adsorption branch. On the right side of Fig.5 gave the size distributions of obtained V-HMSNSs with different concentrations of CTAB (0.0009 M and 0.005). It can be clearly observed that the pore size distributions of these two samples were all very broad in the range of 1 nm to 65 nm. Meanwhile,

In addition, the BET surface area and total volume of obtained V-HMSNSs were all listed in Table 1. It was found that the the BET surface area and total volume of obtained V-HMSNSs were increased as the CTAB concentrations were increased, which should be a result of the different porous structures of V-HMSNSs prepared with different CTAB concentrations. For one thing, the rate of hydrolysis and condensation of VTES can be accelerated with the increase of the concentration of CTAB, For another, the increase of the concentration of CTAB was helpful to form more micelles, and further wrapped by silica spheres, which was in favor of the formation of more pores.

Effect of the amounts of ammonia

Generally hydrolysis of organosilane was a very slow reaction, though acids or bases are used as catalysts. Therefor, It was believed that the hydrolysis and condensation rates of the organosilanes were closely related to the amounts of acids or bases catalysts. In this study, the influence of different amounts of ammonia catalyst at aqueous solution on the formation of V-HMSNSs has been discussed. Fig.6 showed the representative TEM images of the samples prepared under different volumes of ammonia: (A) 1 mL, (B) 2 mL and (C) 3 mL at aqueous solution under CMC value of CTAB. Obviously, hollow-to-solid spheres transition was occurred as the amount of ammonia was increased from 1 mL to 3 mL (Fig.6(A)). It was not difficult to explain that the hydrolysis and condensation rate of vinyltriethoxysilane precursor at aqueous solution may be greatly accelerated at higher ammonia amount, resulting in the formation of a relative larger solid sphere. For instance, CTAB@V-SiO_2

nanocomposite particles with thick shell were formed as the amount of ammonia was increased to 2 mL, as shown in Fig.6(B). Furthermore, the larger solid spheres were obtained as the amount of ammonia was up to 3 mL (Fig.6(C)).

Effect of the volume ratios of alcohol to water

It was well known that ethanol played very important role in the hydrolysis and condensation rate of silane. According to the previously reports, ethanol can greatly promote the the hydrolysis and condensation rates of silane precursor, and this was closely related to the amount of the alcohol.[38] Therefore, in order to further study the influence of ethanol to the formation of V-HMSNSs, effect of the volume ratio of alcohol to water to the formation of V-HMSNSs has been investigated at others conditions fixed, as listed in the Table 2. It was found that no particles were generated as the volume ratio of alcohol to water was increased from 0:50 to 15:35 (Table 2). While the volume ratio of alcohol to water was increased to 20:30, TEM image confirmed that the sample was composed of irregular spherical solid particles with a large average size around 1660 nm (Fig.7(A)), and agglomeration of silica nanoparticles (Fig.7(B)). As the volume ratio of alcohol to water was further increased to 25:25, the part of ellipsoidal silica particles with mesostructure were observed in the TEM image in Fig.7(C). However, there were still some spherical solid particles in the sample (Fig.7(D)). Fig.8 showed the representative N_2 adsorption-desorption isotherms and the corresponding pore size distribution of the samples whose TEM images were displayed in Fig.7(C,D). The BET surface area and total pore volume were relative small about 1.8 $m^2 g^{-1}$ and 0.0028 $cm^3 g^{-1}$, respectively (Table 2), due to the presence of some solid silica spheres. Meanwhile, the corresponding pore size distribution centered at 16.3 nm, and in addition to the mesoporosity, BJH pore size distribution clearly showed that V-HMSNSs also had micropores with diameter centered around 1.8 nm (Fig.8(B)). According to the mechanism of hydrolysis and condensation of vinyltriethoxysilane precursor as following:

Hydrolysis:

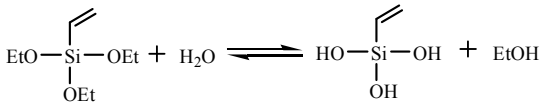

(1)

Condensation:

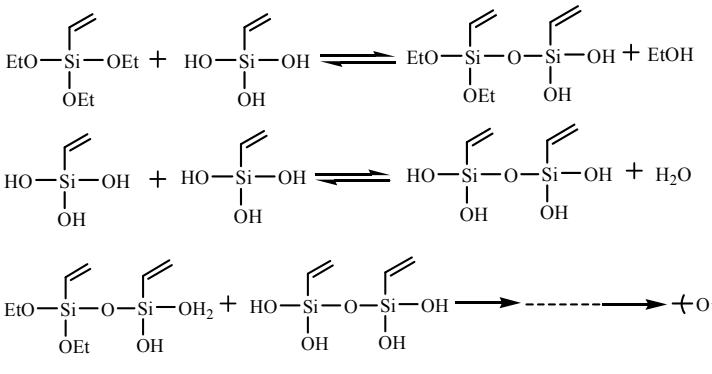

(2)

(3)

suggested that the formation of vinyl functionalized silica nanospheres under the current conditions was mainly dependent on the hydrolysis and condensation rates of vinyltriethoxysilane. Furthermore, the hydrolysis and condensation rates of vinyltriethoxysilane will be affected by the amount of ethanol. It was believed that the hydrolysis and condensation rates of vinyltriethoxysilane precursor may be greatly suppressed under pure water condition or low ratio of alcohol to water. In this study, The results proved that the particles were not obtained until the volume ratio of alcohol to water was up to 20:30. At this point, a few hydrolyzed silanol groups were further condensated into a small silica oligomer before compacting with the CTAB template, solid spheres were thus obtained. While the volume ratio of alcohol to water was further increased to 25:25, the adequate ethanol favored the formation of a large number of hydrolyzed silanol groups, and these hydrolyzed silanol groups may be collided with the CTAB molecules, and further hydrolysis and condensation on the surface of CTAB template before self condensation were occurred. Consequently, V-HMSNSs were synthesized after removing of CTAB template. However, the hydrolysis rate of vinyltriethoxysilane precursor was far faster than that condensation rate when the volume ratio of alcohol to water was beyond 25:25, such as 40:10 or 50:0, only hydrolyzed silanol groups or silica oligomers were formed. So no particles were observed (Table 2).

4. Conclusions

A facile and low cost method has been developed for the synthesis of vinyl funcitonalized hollow mesoporous silica nanospheres under a mild condition. The vinyl functionalized hollow mesostructure silica nanospheres and nanorods can be obtained by adjusting the cetyltrimethylammonium bromide concentration at aqueous solution under low ammonia concentration. Vinyl functionalized hollow

mesostructure silica nanospheres and nanorods were formed at the critical micelle concentration value of the cetyltrimethylammonium bromide or little higher this value. Meanwhile, the hollow mesostructure nanospheres can also be prepared under similar condition except the addition of alcohol, and the results showed that the vinyl functionalized hollow mesostructure silica nanospheres can be obtained only when the volume ratio of alcohol to water was 25:25. In addition, vinyl funcitonalized hollow mesoporous silica nanospheres are expected to be used as adsorption as well as microencapsulation.

Acknowledgements

This work was partially supported by the National Natural Science Foundation of China (Grants 51273155). This work was also financially supported by the GuangDong Well-SilicaSol Co., LTD, China.

References

1 H. Djojoputro, X. F. Zhou, S. Z. Qiao, L. Z. Wang, C. Z. Yu and G. Q. Lu, *J. Am. Chem. Soc.,*2006, **128,** 6320.

2 F. Hoffmann, M. Cornelius, J. Morell and M. FrÖba, *Angew. Chem. Int. Ed.,* 2006, **45,** 3216.

3 J. Y. Yuan, Y. Y. Xu, A. Walther, S. Bolisetty, M. Schumacher, H. Schmalz, M. Ballauff and A. H. Müller, *Nat. Mater.,* 2008, **7,** 718.

4 J. Liu, S. Y. Bai, H. Zhong, C. Li and Q. H. Yang, *J. Phys. Chem. C,* 2010, **114,** 953.

5 A. E. Kadib, N. Katir, M. Bousminaac and J. P. Majoral, *New J. Chem.,* 2012, **36,** 241.

6 M. Mandal and M. Kruk, *Chem. Mater.,* 2012, **24,** 123.

7 X. B. Li, Y. Yang and Q. H. Yang, *J. Mater. Chem. A,* 2013, **1,** 1525.

8 J. S. Beck, J. C. Vartuli, W. J. Roth, M. E. Leonowicz, C. T. Kresge, K. D. Schmitt, C. T. W. Chu, D. H. Olson, E. W. Sheppard, S. B. McCullen, J. B. Higgins and J. L. Schlenker, *J. Am. Chem. Soc.,* 1992, **114,** 10834.

9 C. T. Kresge, M. E. Leonowicz, W. J. Roth, J. C. Vartuli and J. S. Beck, *Nature,* 1992, **359,** 710.

10 S. Inagaki, S. Guan, Y. Fukushima, T. Ohsuna and O. Terasaki, *J. Am. Chem.*

Soc., 1999, **121,** 9611.

11 B. J. Melde, B. T. Holland, C. F. Blanford and A. Stein, *Chem, Mater.,* 1999, **11,** 3302.

12 T. Asefa, M. J. MacLachlan, N . Coombs and G. A. Ozin, *Nature,* 1999, **402,** 867.

13 A. M. Liu, K. Hidajat, S. Kawi and D. Y. Zhao, *Chem. Commun.,* 2000, 1145.

14 A. Matsumoto, K. Tsutsumi, K. Schumacher and K. K. Unger, *Langmuir,* 2002, **18,** 4014.

15 D. R. Radu, C.-Y. Lai, J. W. Wiench, M. Pruski and V. S.-Y. Lin, *J. Am. Chem. Soc.,* 2004, **126,** 1640.

16 S. L. Burkett, S. D. Sims and S. Mann, *Chem. Commun.,* 1996, 1367.

17 M. H. Lim, C. F. Blanford and A. Stein, *J. Am. Chem. Soc.,* 1997, **119,** 4090.

18 R. Anwander, I. Nagl and M. Widenmeyer, *J. Phys. Chem. B,* 2000, **104,** 3532.

19 K. Yao, Y. S. Imai, L. Y. Shi, A. M. Dong, Y. Adachi, K. Nishikubo, E. Abe and H. tateyama. *J. Colloid Interface Sci.,* 2005, **285,** 259.

20 Q. Wei, Z. R. Nie, Y. L. Hao, Z. X. Chen, J. X. Zou and W. Wang, *Mater. Lett.,* 2005, **59,** 3611.

21 M. Choi, F. Kleitz, D. Liu, H. Y. Lee, W. S. Ahn and R. Ryoo, *J. Am. Chem. Soc.,* 2005, **127,** 1924.

22 Y. S. Lin, S. H. Wu, C. T. Tseng, Y. Hung, C. Chang and C. Y. Mou, *Chem. Commun.,* 2009, 3542.

23 P. Zarabadi-Poor, A. Badiei, B. D. Fahlman, P. Arab, and G. M. Ziarani, *Ind. Eng. Chem. Res.* 2011, **50,** 10036.

24 L. Han, Q. R. Chen, Y. Wang, C.B.Gao, S. A. Che, *Microporous Mesoporous Mater.,* 2011, **139,** 94.

25 R. Vathyam, E. Wondimu, S. Das, C. Zhang, S. Hayes, Z. M. Tao and T. Asefa, *J. Phys. Chem. C,* 2011, **115,** 13135.

26 B. Liu, E. W. Yan, X. Zhang, X. L. Yang and F. Bai. *J. Colloid Interface Sci.,* 2012, **369,** 144.

27 H. Yoshitake, *New J. Chem.* 2005, **29,** 1107.

28 I.A. Rahman, M. Jafarzadeh, C.S. Sipaut, *Ceram. In.,* 2009, **35,** 1883.

29 Y. Naka, Y. Komori, H. Yoshitake, *Colloids Surf., A,* 2010, **361**, 162.

30 Q. S. Huo, D. I. Margolese, U. Ciesla, D. G. Demuth, P. Y. Feng, T. E. Gier, P. Sieger, S. A.Firouzi, B. F. Chmelka, F. SchÜth and G. D. Stucky. *Chem. Mater.,*

1994, **6,** 1176.

31 Q. S. Huo, D. I. Margolese, U. Ciesla, P. Y. Feng, T. E. Gier, P. Sieger, R. Leon, P. M. Petroff, F. SchÜth and G. D. Stucky. *Nature,* 1994, **368,** 317.

32 W. Li, Y. C. Han, J. L. Zhang, L. X. Wang and J. Song. *Colloid J.,* 2006, **68,** 304.

33 M. Bielawska, A. Chodzińska, B. Jańczuk, A. Zdziennicka. *Colloids Surf., A,* 2013, **424,** 81.

34 H. T. Pu, X. Zhang, J. J. Yuan and Z. L. Yang, *J. Colloid Interface Sci.,* 2009, **331,** 389.

35 Z. Meng, C. Y. Xue, Q. H. Zhang, X. Yu, K. Xi, X. Jia, *Langmuir,* 2009, **25,** 7879.

36 Z. Q. Wu, H. Chen, X. L. Liu, Y. Zhang, D. Li, H. Huang, *Langmuir,* 2009, **25,** 2900.

37 I. O. Ucar , M. D. Doganci, C. E. Cansoy, H. Y. Erbil, I. Avramova, S. Suzer, Appl. Surf. Sci., 2011, **257,** 9587.

38 W. Stöber, A. Fink, *J. Colloid Interface Sci.,*1968, **26,** 62.

Scheme 1 Schematic illustration of one step method based on the soft template route for preparing V-HMSNSs

Table Captions

Table 1 Physicochemical parameters of the samples synthesized at different concentrations of CTAB under pure water system at 25 ^{o}C.

Table 2 Physicochemical parameters of the samples synthesized at different volume ratios of alcohol to water at 25 ^{o}C.

Table 1 Physicochemical Parameters of the Samples Synthesized using Different Concentrations of CTAB at room temperature (25 ^{o}C)

No.	water (mL)	CTAB concentrations (M)	average particles size (nm)	BET surface area ($m^2 g^{-1}$)	total pore volume ($cm^3 g^{-1}$)
1	50	0.01	no particles	-	-
2	50	0.008	no particles	-	-
3	50	0.005	2070	113	0.24
4	50	0.0009	512	14	0.019
5	50	0.0005	510	solid spheres	solid spheres

Table 2 Physicochemical Parameters of the Samples Synthesized using Different Alcohol-Water Ratios at room temperature (25 ^{o}C)

No.	CTAB concentration (M)	alcohol/water volume ratio (v:v)	average particles size (nm)	BET specific surface area ($m^2 g^{-1}$)	total pore volume ($cm^3 g^{-1}$)	pore size (nm)
1	0.01	0:50	no particles	-	-	-
2	0.01	15:35	no particles	-	-	-
3	0.01	20:30	1660	solid spheres	solid spheres	solid spheres
4	0.01	25:25	3476	1.8	0.0028	6.1
5	0.01	40:10	no particles	-	-	-
6	0.01	50:0	no particles	-	-	-

Figure Captions

Fig.1 TEM images of V-HMSNSs synthesized with different concentrations of CTAB: (A, B) = 0.0005 M, (C, D)= 0.0009 M and (E, F)= 0.005 M at aqueous solution.

Fig.2 FTIR spectra of (a) CTAB, (b) CATB@V-SiO_2, (c) V-HMSNs and (d) pure silica nanospheres

Fig.3 TGA analysis of (a) pure silica nanoparticles and (b) V-HMSNs

Fig.4 XPS analysis of (a) V-HMSNs and (b) pure silica nanoparticles

Fig.5 Nitrogen adsorption (■) and desorption (●) isotherm curves and corresponding pore size distributions of V-HMSNSs synthesized with different concentrations of CTAB: (A, B)= 0.0009 M and (C, D)= 0.005 M at aqueous solution.

Fig.6 TEM images of V-HMSNSs synthesized with different volumes of NH_3: (A) = 1 mL, (B)= 2 mL and (C) = 3 mL at aqueous solution.

Fig.7 TEM images of V-HMSNSs synthesized with different volume ratios of alcohol to water: (A,B) 20:30 and (C,D) = 25:25.

Fig.8 (A) Nitrogen adsorption (■) and desorption (●) isotherm curve and (B) corresponding pore size distribution of V-HMSNSs synthesized with volume ratio of alcohol to water for 25:25.